

## A new method to estimate resistivity distribution of shaly sand reservoirs using new seismic attributes

NUR FARHANA SALLEH<sup>1,2,\*</sup>, MAMAN HERMANA<sup>1,2</sup>, DEVA PRASAD GHOSH<sup>1</sup>

<sup>1</sup> Center of Excellence in Subsurface Seismic Imaging & Hydrocarbon Prediction (CSI), Universiti Teknologi PETRONAS, 32610 Bandar Seri Iskandar, Perak Darul Ridzuan, Malaysia  
<sup>2</sup> Department of Geosciences, Universiti Teknologi PETRONAS, 32610 Bandar Seri Iskandar, Perak Darul Ridzuan, Malaysia  
\* Corresponding author email address: nur\_17006583@utp.edu.my

**Abstract:** A subsurface resistivity model is important in hydrocarbon exploration primarily in the controlled-source electromagnetic (CSEM) method. CSEM forward modelling workflow uses resistivity model as the main input in feasibility studies and inversion process. The task of building a shaly sand resistivity model becomes more complex than clean sand due to the presence of a shale matrix. In this paper, a new approach is introduced to model a robust resistivity property of shaly sand reservoirs. A volume of seismic data and three wells located in the K-field of offshore Sarawak is provided for this study. Two new seismic attributes derived from seismic attenuation property called SQp and SQs are used as main inputs to predict the volume of shale, effective porosity, and water saturation before resistivity estimation. SQp attribute has a similar response to gamma-ray indicating the lithological variation and SQs attribute is identical to resistivity as an indicator to reservoir fluids. The petrophysical predictions are performed by solving the mathematical step-wise regression between the seismic multi-attributes and predicted petrophysical properties at the well locations. Subsequently, resistivity values are estimated using the Poupon-Leveaux (Indonesia) equation, an improvised model from Archie's to derive the mathematical relationship of shaly sand's resistivity to the volume and resistivity of clay matrix in shaly sand reservoirs. The resistivity modeled from the predicted petrophysical properties distributed consistently with sand distribution delineated from SQp attribute mainly in southeast, northeast, and west regions. The gas distribution of the net sand modeled by 5% and 90% of gas saturation scenarios also changed correspondingly to SQs attribute anomaly indicating the consistent fluid distribution between the modeled resistivity and SQs attribute.

**Keywords:** Shaly sand reservoir, Poupon-Leveaux model, resistivity

### INTRODUCTION

Building a reliable resistivity model is an imperative step prior to electromagnetic feasibility studies (Werthmüller *et al.*, 2013). The reliability of a resistivity model is determined by the corresponding resistivity change with the lithological variation. Nevertheless, resistivity property modelling has an additional challenge for a shaly sand reservoir due to the low resistivity contrast to its overburden lithology. The presence of clay minerals in shaly sand retains more water thus suppress the measurement of electrical resistivity of a shaly sand reservoir (Fazao *et al.*, 2019). Archie's Law mathematically defines the resistivity of clean sand to its water saturation and porosity (Archie, 1942). However, in cases of shaly sand reservoirs, Archie's model overestimates the water saturation and gives rise to pessimistic interpreted hydrocarbon saturation. To accommodate clay's properties into a reservoir's resistivity calculation, several models were established based on the modification of Archie's equation. The Indonesia model (Leveaux & Poupon, 1971) is one of the modified models that has been widely used to define the mathematical relationship between the resistivity of shaly sand to its clay properties. It takes into account the volume

and resistivity of the shale matrix to estimate hydrocarbon saturation in shaly sand reservoirs more accurately.

Therefore, prior to shaly sands resistivity modelling, the Indonesia model requires prerequisite inputs of petrophysical properties in volume such as effective porosity, the volume of shale matrix, and water saturation. It is crucial to model the petrophysical volume property consistently to lithological and fluid variations. To date, the reservoir's property extrapolation method using geostatistical algorithms such as Gaussian and Kriging processes manifest high distribution uncertainty when the drilling well numbers are limited in a hydrocarbon exploration field. Consequently, the modeled property has a poor lithological and fluid distribution consistency mainly in a region of kilometers away from the well location which has less reservoir property information.

The new workflow demonstrated in this paper is to improve the distribution consistency of the shaly sands resistivity model. The improvement is achieved by integrating the new seismic attenuation attributes in petrophysical property prediction prior to resistivity estimation. The new seismic attenuation attributes are known as SQp and SQs, which are used to delineate the lithology and fluid distribution

from the previous works (Hermana *et al.*, 2016; 2018). The work in this paper has extended the application of these attributes by including them in the prediction process to model the petrophysical properties of shaly sand reservoirs. The geostatistical extrapolation method is replaced with the predictive method where it utilizes seismic multi-attributes volumes to extrapolate and control the continuity of the modeled reservoir property mainly away from the wells. The upcoming section will discuss in detail the study area, data scopes, methodology, and finally, the results of the modeled petrophysical property and resistivity of the shaly sand reservoir in the K-field are comprehensively discussed.

**GEOLOGICAL SETTING OF STUDY AREA**

K-field is a gas field located in the Central Luconia region approximately 200,000 km from Bintulu MLNG Plant as shown in Figure 1. The hydrocarbon trap comprises a combination of stratigraphic and structural play (Vahrenkamp, 1998). Two main thin gas reservoirs are interpreted from the seismic data with sand thickness ranging between 23 meters to 28 meters (Zailani & Ghosh, 2017). From shallow to a deeper section, they are denoted as Sand-1 and Sand-2 in a setting of very gentle structure and stratigraphic layering. The gas generation originated from Cycle-1 and Cycle-II group source rocks and migrated through deep-rooted faults to Cycle V and Cycle VI sand reservoirs (Vahrenkamp, 1998; Joseph *et al.*, 2019).

The characterized sand is originated from two possible depositional environments which are either turbidites or holomarine inner to outer neritic bathyal environment by the coarsening upward trend sand size and texture (Coleou *et al.*, 2003; Zailani & Ghosh, 2017).

**DATA SCOPE**

Three wells are provided for this study located within the surveyed seismic area consisting of exploration and appraisal wells. From northwest to southeast, the wells are denoted by K-3, K-1, and K-2 respectively as shown in Figure 1. The available measured logs include gamma-ray, neutron-porosity, density, resistivity, sonic, and other interpreted petrophysical properties such as water saturation, the volume of shale, and effective porosity. All logs are utilized to identify the reservoir intervals which will be discussed in the results section.

A volume of post-stack seismic data is also provided of an area of 150 km<sup>2</sup> with 1600 ms of maximum travel time. The 3D seismic data is acquired in 2004 with a good data quality where most major markers above 2.5 seconds show a clear lateral continuity and discontinuity at fault locations (Ghosh *et al.*, 2014). Structural and stratigraphic features identified from the seismic data and gas reservoirs demonstrated very strong AVO anomalies at major reservoir zones from the full stacking volume at 40 Hz of dominant frequency (Shahud *et al.*, 2011).

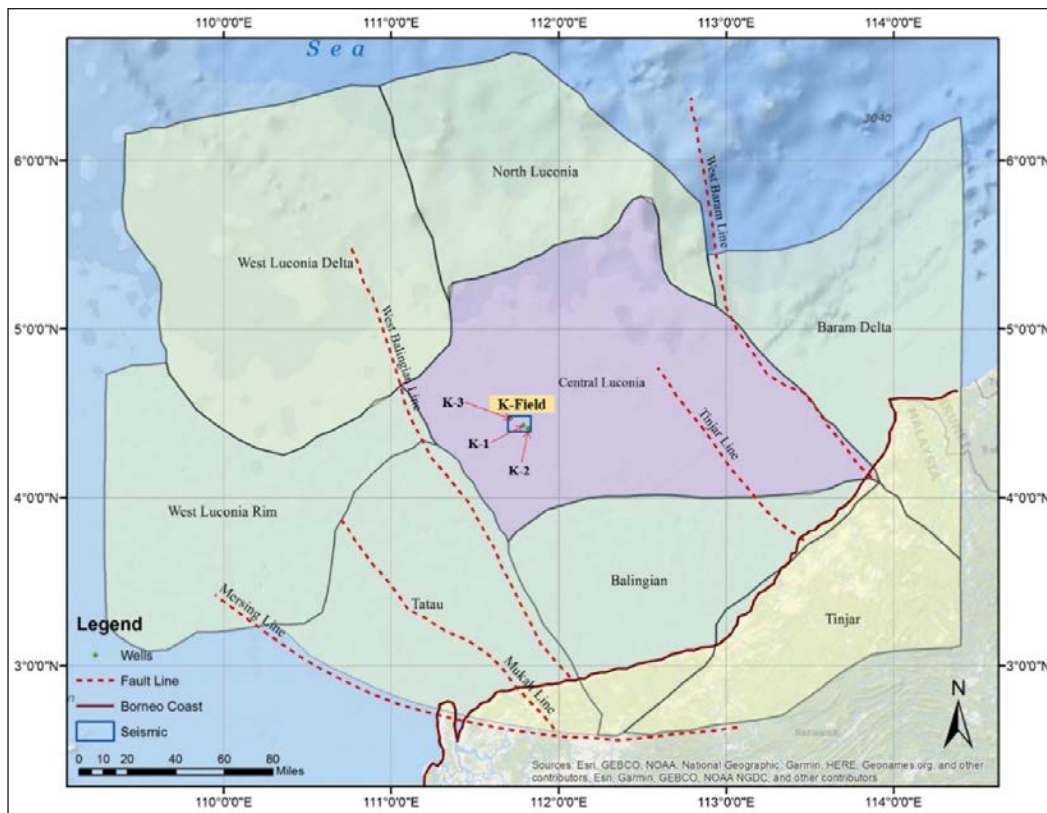


**Figure 1:** Location of K-1, K-2 and K-2 wells within the surveyed seismic geometry.

**METHODOLOGY**

A novel method is presented in this study by incorporating new seismic attributes, SQp and SQs in petrophysical volume prediction before resistivity volume estimation. This method produces a detailed petrophysical property distribution that is consistent with the anomalies delineated from the seismic attributes. Next, the predicted properties are used as the main input to model the resistivity volume using the Indonesia model’s equation. A detailed sequence of the workflow is illustrated in Figure 2 and further elaboration of each process is discussed in the following subsections.

**Well logs analysis**

The provided well logs such as gamma-ray, neutron-porosity, density, and resistivity logs are analyzed to identify the sand and gas intervals. The interpreted petrophysical property logs such as water saturation, shale fraction, and effective porosity are evaluated to assess the quality of the sand reservoirs. Gamma-ray log differentiates sand intervals from the shale formations which is indicated by low gamma-ray reading due to the low clay content. The gas zone is identified by discerning the high resistivity log values and crossover zones by plotting neutron-porosity and density logs together. To determine the net sand, each interpreted sand interval is extracted based on the petrophysical cut-off

values of effective porosity ≥ 10%, water saturation ≤ 50% and volume of shale ≤ 60%.

Two new seismic attributes, SQp and SQs are generated at the well location by validating the attribute response to gamma-ray and resistivity log respectively. SQp attribute practically has a similar lithological response to gamma-ray log and SQs attribute on the other hand is similar to resistivity log which is highly affected by fluid type and saturation. These attributes are derived from the attenuation property through rock physics approximation which can be presented through the following equations (Hermana *et al.*, 2016):

$$SQ_p = \frac{5}{6} \frac{1}{\rho} \frac{\left(\frac{M}{G}-2\right)^2}{\left(\frac{M}{G}-1\right)} \tag{1}$$

$$SQ_s = \frac{10}{3} \frac{1}{\rho} \frac{\left(\frac{M}{G}\right)}{\left(\frac{3M}{G}-2\right)} \tag{2}$$

Where M/G is the ratio of bulk and shear modulus that can be approximated from P-wave and S-wave velocity ratio and ρ is the density of the rock.

**Pre-stack seismic inversion**

Seismic inversion is a process of extracting the interface of formation seismic reflectivity and inverting them into elastic rock property layers. In a pre-stack seismic inversion, seismic gathers of different angle ranges are inverted to produce P-impedance, S-impedance, and density. Subsequently, the inverted elastic models are utilized to generate the SQp and SQs volume attributes based on equations (1) and (2).

Well to seismic tie is an important task before the inversion process as it calibrates lithological interface from wells to seismic traces as well as optimizing the time-to-depth conversion process. This process is described by stretching or squeezing zero-offset well synthetic traces by correlating them to the similar seismic events from the extracted composite seismic traces nearby the well. A good correlation of a seismic-well tie is validated by the higher cross-correlation coefficient value.

Partial seismic gathers consisted of the near, middle, and far angles ranging from 5° to 40° used as the primary data input in the inversion process. The low-frequency initial models of P-impedance, S-impedance, and density are built by inputting the interpreted seismic horizons and corrected sonic and density logs. Three wavelets are extracted from each partial gathers where the angle of the gathers ranging from 5° to 15°, 15° to 25°, and 25° to 40° for near, middle, and far angles respectively. Inversion analysis is performed on inverted seismic models at the well location as quality control to obtain optimum inversion parameters before seismic volume inversion. The inversion parameters such as regression coefficient, background ratio of Vp/Vs, pre-

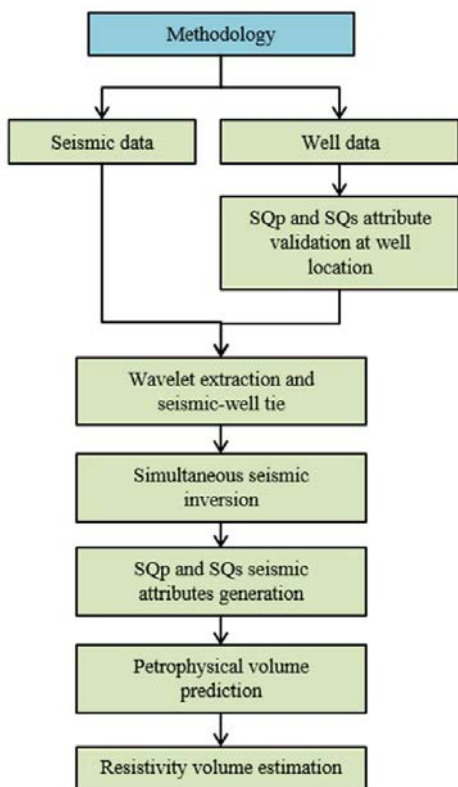


**Figure 2:** Flowchart of the new approach to estimate resistivity of shaly sand reservoirs.

whitening, and muted dead traces are optimized to minimize the error values of inverted P-impedance, S-impedance, and density to original logs. The regression coefficients are determined by cross-plotting both the inverted logarithmic S-impedance and P-impedance at the well location. The optimum parameters are obtained by evaluating the lowest error and highest correlation values of each inverted model which is used in the final seismic volume inversion run.

**Petrophysical property volume prediction**

The volume of shale, effective porosity, and water saturation are the primary parameters controlling the resistivity values of shaly sands as defined in the Indonesia model. Hence, providing these three petrophysical properties in the volume are prerequisite inputs before resistivity volume calculation. In this study, the petrophysical property volumes are generated using a predictive method based on a step-wise regression algorithm.

Each property is predicted independently as the seismic multi-attributes dataset used in their training computations are different subjected to their mathematical relationship to formation elastic property. A set of final multi-attributes are selected to predict each petrophysical property tabulated in Table 1. SQp attribute is incorporated to predict effective porosity and volume of shale as these petrophysical properties showed a good relationship to rock acoustic impedance. The water saturation is predicted by adding the SQs attribute as this is an attribute to fluid indicator similar to the resistivity log as discussed previously. The training process worked by finding the best attribute set of each predicted property to solve the step-wise linear regression function by determining the weight coefficient of each seismic attribute extracted at the well location. The final attribute set for each property prediction is ranked based on the declining average error. The final attribute

set is selected for the final prediction based on the lowest average error and highest correlation values.

**Resistivity volume modelling**

The resistivity volumes are computed by inputting each predicted petrophysical volume property obtained from the previous method into the Indonesia model’s equation. The resistivity volumes are generated for two gas scenario cases, 5% and 90% of gas saturation to represent the low and high gas saturation cases respectively. The resistivity calculation of each gas scenario was conditioned by the petrophysical cut-off values of effective porosity  $\geq 10\%$ , water saturation  $\leq 50\%$  and volume of shale  $\leq 60\%$ .

**RESULTS AND DISCUSSION**

**Well logs interpretation**

In this paper, only interpretation of K-2 well logs is discussed followed by other results located near to K-2 well location. The identification of sand and gas intervals is done by evaluating gamma-ray, density, porosity, and resistivity logs as well as petrophysical logs such as water saturation and volume of shale. K-2 well is located southeast of the seismic area shows the presence of two stacking thin shaly sand reservoirs as shown in Figure 3. The first sand is identified at a TVD of 704 meters with a thickness of 16 meters. The second sand is located 20 meters below the first sand at a TVD of 740 meters with a thickness of 20 meters.

The sand layers are distinguished from shale formation by low gamma-ray and SQp values. The crossover of density and neutron-porosity logs suggests a gas zone sand and is also indicated by the increase of SQs attribute. However, the resistivity contrast is insignificant at the top and base reservoir due to the high volume of shale matrix ranging from 50% to 75% within the reservoir intervals. The high content of shale suppresses the resistivity readings due to

**Table 1:** Final seismic attributes used in petrophysical property volume prediction.

|                                            | Volume of shale, Vshale             | Effective porosity, $\Phi_e$        | Water saturation, Sw          |
|--------------------------------------------|-------------------------------------|-------------------------------------|-------------------------------|
| Number of final multi attributes transform | 5                                   | 4                                   | 5                             |
| Minimum training error                     | 0.0907                              | 0.0542                              | 0.0623                        |
| Minimum validation error                   | 0.1213                              | 0.0585                              | 0.0980                        |
| Final multi attributes transform dataset   | (Filter 15/20-25/30)*Inverted $I_p$ | Integrated Absolute*SQp             | Filter 15/20-25/30            |
|                                            | (Filter 25/30-35/40)*SQp            | (Filter 15/20-25/30)*Inverted $I_p$ | Integrated Absolute Amplitude |
|                                            | Instantaneous Frequency*SQp         | Integrate*SQp                       | Filter 5/10-15-20             |
|                                            | Quadrature Trace*Inverted $I_p$     | (Filter 15/20-25/30)*SQp            | Apparent Polarity             |
|                                            | (Filter 35/40-45/50)*SQp            |                                     | I/SQs                         |

the conductive property of clay minerals thus low resistivity contrast is observed from the log. The average water saturation of the reservoirs is estimated at 55% which is equivalent to 45% of gas.

**Pre-stack seismic inversion**

Pre-stack seismic inversion is carried out to delineate the lateral distribution of shaly sand elastic property as observed in the K-2 well. Two layers of reservoirs are identified from the inverted models located in between interpreted

Horizon 1 and Horizon 2. The inverted elastic properties are well-matched with the stacking sands identified in the K-2 well as shown in Figure 4. The reservoir intervals are indicated by low inverted Vp/Vs and SQp response which is correlated to the measured low Vp/Vs and SQp response in the K-2 well logs. The gas intervals are delineated from the SQs attribute showing the increase of SQs values within the sand intervals. The high SQs response of the gas layers is also well matched with the derived SQs response in the K-2 well log as shown in Figure 4.

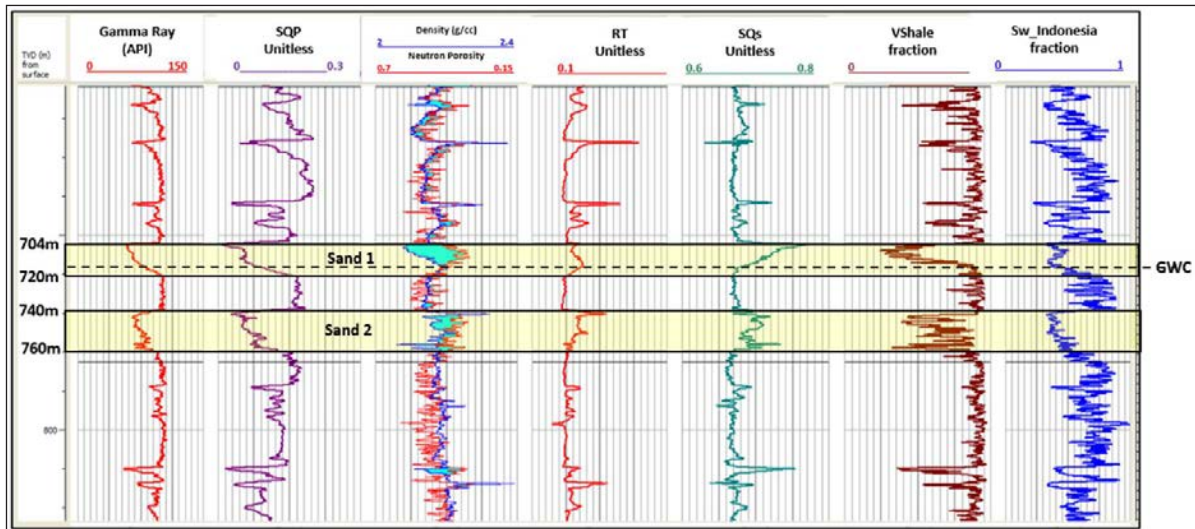


Figure 3: Sand-1 and Sand-2 interpreted from K-2 well.

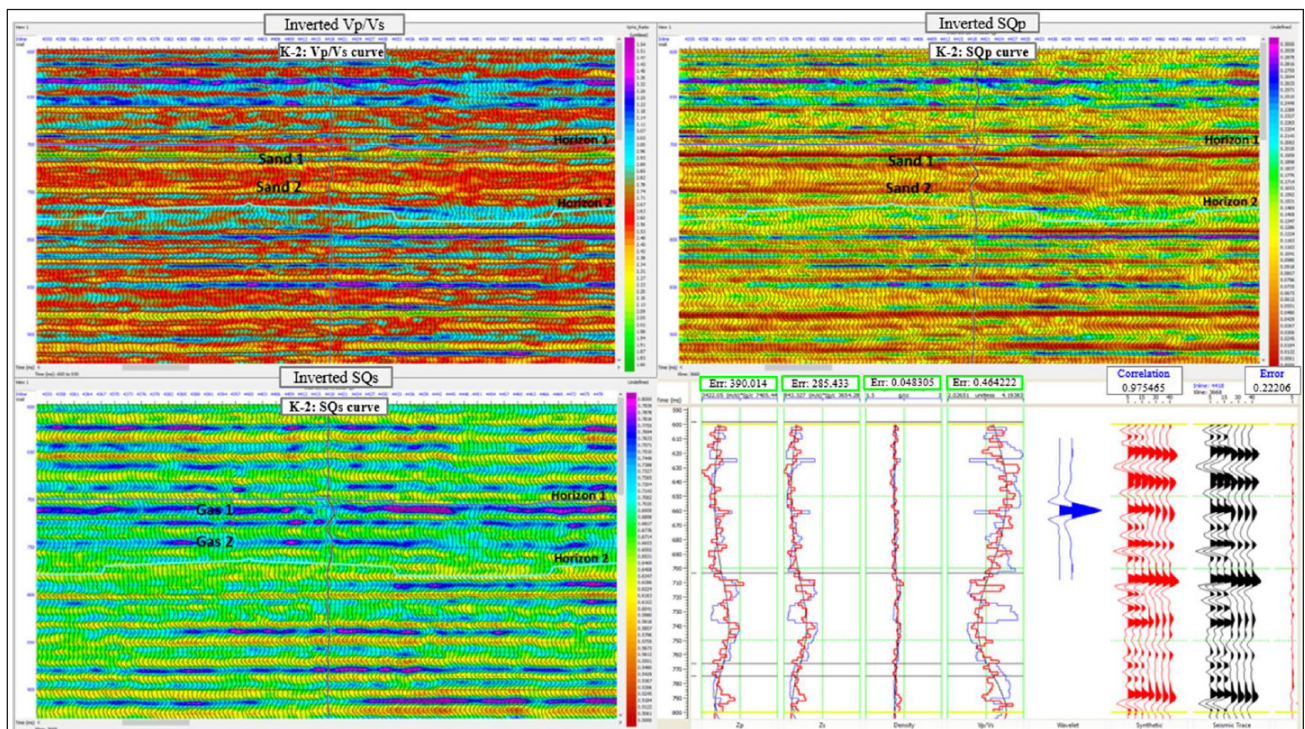


Figure 4: Vp/Vs inverted model (upper left), SQp attribute (upper right), SQs attribute (lower left) and inverted P-impedance, S-impedance, density and Vp/Vs in red logs and original logs in black. Inverted and real seismic traces are shown in red and black colored traces respectively.

The inversion analysis at the K-2 well location showed a good fitting between the inverted model and original log for P-impedance, S-impedance, density, and Vp/Vs as shown in Figure 4. The final synthetic gathers in red traces generated from the inversion show a good cross-correlation to the extracted seismic traces in black with a value of 0.975 and an RMS error of 0.222. These are the optimum parameters obtained by inverting seismic traces at the K-2 well location and are applied to invert the whole seismic volume.

**Petrophysical volume prediction**

The application of the predictive method produces reliable and consistent petrophysical distributions estimated

for the volume of shale, effective porosity, and water saturation. A good distribution consistency is crucial to generate robust resistivity models to represent shaly sand reservoir distribution in the K-field.

Two interval layers of the low volume of shale are identified located at the same depth as the stacking sands interpreted in the K-2 well. These layers are also correlated to the low volume of shales from the measured log in the K-2 well as shown in Figure 5. The predicted volume of shale for all wells used in the training stage shows a good fitting between the predicted log in red and the original log in black as shown in Figure 5. The final prediction is validated by a cross-correlation value of about 0.64 and an RMS error of 0.12.

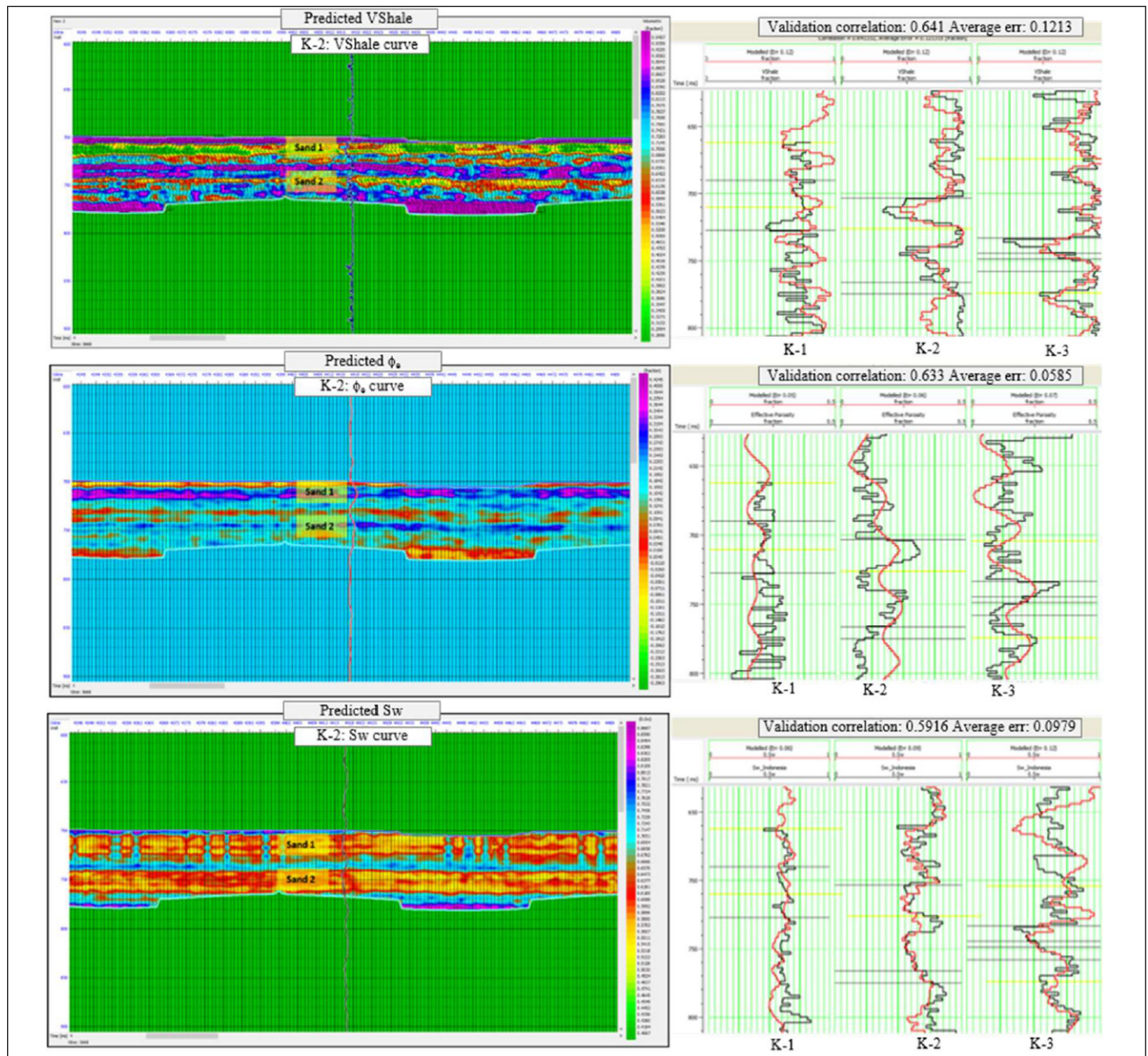


**Figure 5:** Predicted volume of shale (upper left), effective porosity (middle left) and water saturation (lower left) image respectively. The cross correlation and average error values in right hand side are shown for each predicted property in red logs and original measurement in black logs for all training wells used in the prediction.

The predicted effective porosity shows high porosity values located at the same depth interval with the stacking sands identified in the K-2 well as shown in Figure 5. These high porosity layers also coincide with the layers of the low volume of shale discussed previously implies the sand layers lateral consistency from the predicted properties. The final validation cross-correlation of the predicted effective porosity is estimated around 0.63 with an RMS error of 0.06 as shown in Figure 5.

The final predicted petrophysical property in this study is water saturation as one of the input parameters to calculate the resistivity in volume based on the Indonesia model. There are two layers with low water saturation and well-matched with the interpreted water saturation log in the K-2 well as shown in Figure 5. The low water saturation within the sand intervals implies gas-filled porosity and laterally consistent with the sand layers with high effective porosity and low volume of shale predicted previously. The final predicted water saturation produces the validation cross-correlation of about 0.59 with an RMS error of around 0.09 as shown in Figure 5.

A cross-checking of the distribution consistency is done simultaneously to all the predicted petrophysical properties at a selected reservoir depth. This is to ensure a consistent shaly sand layer distribution by observing the distribution of each predicted petrophysical property as an important quality control before resistivity estimation. Figure 6 displayed a

slice of each predicted petrophysical property at a depth 710 meters below the seafloor. The shaly sand reservoir is consistently distributed in the southeast (a), northeast (b), and west (c) in red-colored regions indicated by the low volume of shale, a high value of effective porosity, and low value of water saturation. The distribution pattern is also cross-checked on the SQp attribute at the same depth where similar anomaly patterns are also shown in a, b, and c regions. The regions with high SQp values are a lithological indicator of high sand content anomalies which previously cross-validated with the low volume of shale, high effective porosity, and low water saturation.

**Modelled resistivity volume**

The modelled resistivity volume shows consistent resistivity distributions at a depth of 710 meters for 5% and 90% of gas saturation cases as shown in Figure 7. At 5% of gas, low resistivity distributions are observed in southeastern (a), northeastern (b), and western (c) part of the study area indicating conductive reservoirs which are filled by 95% of brine. The conductive anomalies coincide with the gas sand distribution regions delineated from the SQp and SQs attributes shown by low SQp and high SQs values within similar vicinities. The high SQs values in Figure 7 in these regions are the in-situ gas before the gas replacement of 5% and 90% of gas. At 90% of gas, high resistive regions are also observed in the southeast

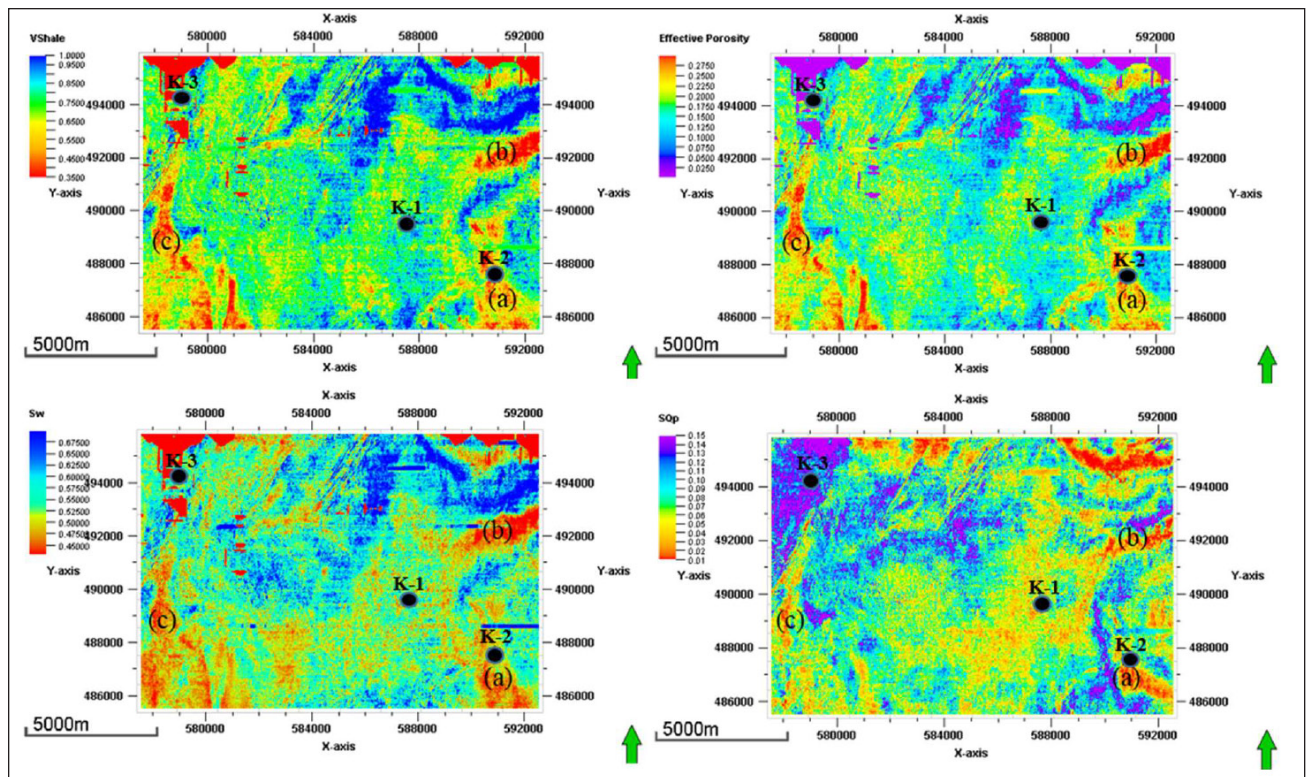


**Figure 6:** A map view of volume of shale (upper left), effective porosity (upper right), water saturation (lower left) and SQs attribute (lower right) at depth of 710 meter below seafloor.

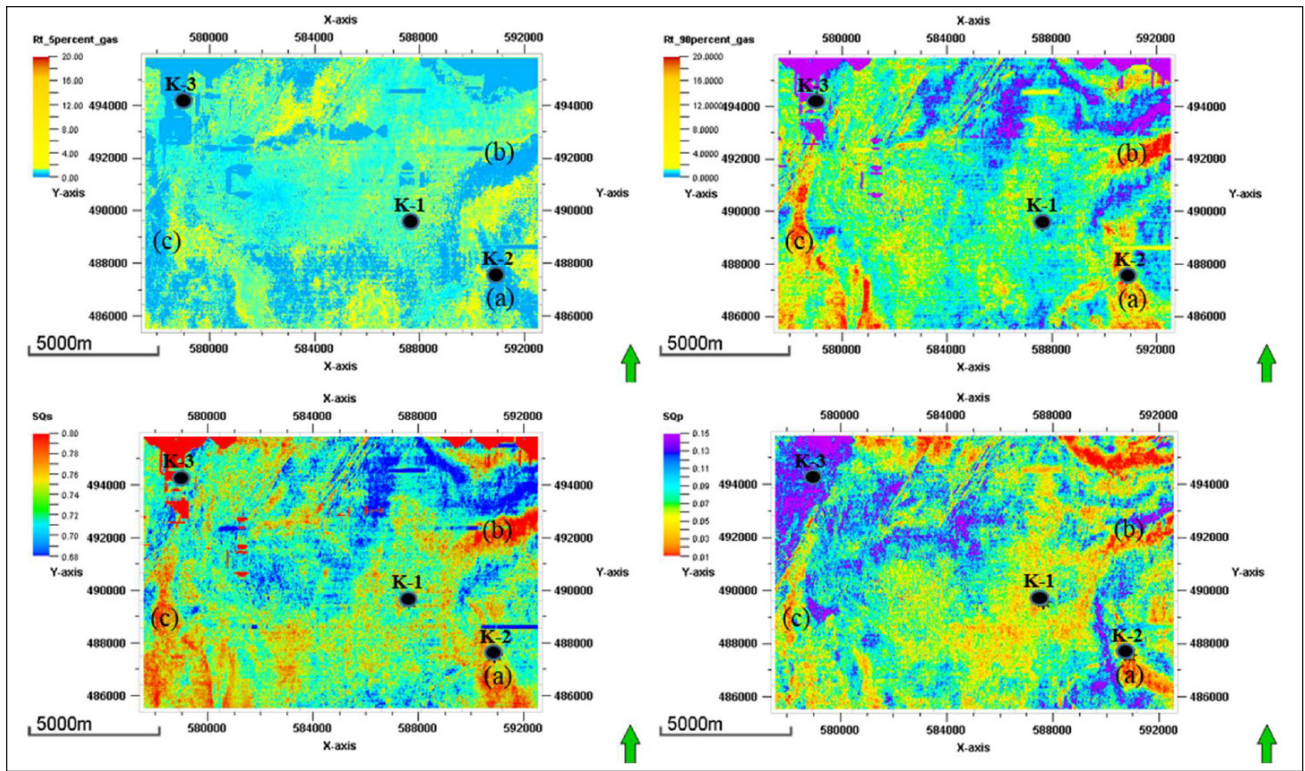


Figure 7: Upper left and upper right images showing resistivity distribution at depth of 710 meter for 5% of gas and 90% of gas respectively. Lower left image showing SQp attribute and lower lower left image showing SQs attribute at similar depth.

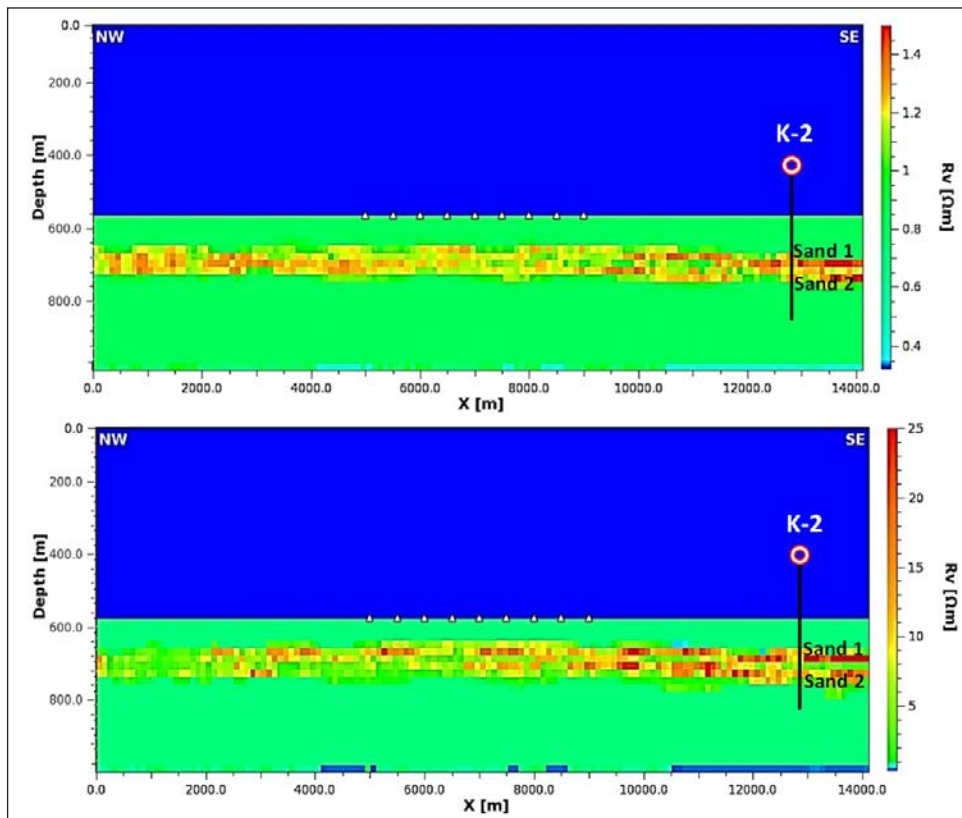


Figure 8: A cross-section of estimated resistivity for 5% of gas saturation in the upper image and 90% of gas saturation in the lower image crossing over K-2 well location.

(a) and northeast (b), and west (c) similar to the SQp and SQs anomalies distribution patterns discussed previously. The estimated resistivity of the sand layers for both gas cases is also correlated to the resistive stacking sand layers identified in the K-2 well located in the southeast of the study area as shown in Figure 8. The consistent distribution of the modeled resistivity to the SQp and SQs seismic attributes and their good correlation to the measured resistivity logs are crucial as quality control to validate the new method introduced in this study which potentially can be applied to model resistivity of shaly sand reservoirs in other areas.

### CONCLUSIONS

This paper presented a new approach to model the resistivity distribution of shaly sand reservoirs by incorporating two new seismic attributes derived from rock attenuation property. The resulting resistivity is laterally consistent with the shaly sand distribution delineated from the new seismic attributes, predicted petrophysical properties as well as measured resistivity at the well location. Through this new approach, the authors have extended the usage of new seismic attributes as volumetric guides to control the continuity of the petrophysical property during the prediction process prior to shaly sand resistivity modelling. A detailed resistivity estimation of a shaly sand reservoir is crucial as this type of reservoir usually has low resistivity in contrast to its overburden due to the high content of shales. Thus, taking into account the shale property into the resistivity estimation will lead to the robust production of the shaly sand resistivity model.

### ACKNOWLEDGEMENTS

The authors would like to extend their appreciation to the Center of Seismic Imaging (CSI) from Universiti Teknologi PETRONAS for providing funding for this study and CGG Malaysia for a contribution of geophysical academic software. The authors are also grateful for the insightful comments by the professional reviewers provided by the Geological Society of Malaysia (GSM) to ensure the quality content of this research work.

### REFERENCES

- Archie, G.E., 1942. The Electrical Resistivity Log as an Aid in Determining Some Reservoir Characteristics. *Petroleum Technology*, T.P(1422), 54–62.
- Coleou, T., Poupon, M. & Azbel, K., 2003. Unsupervised seismic facies classification : A review and comparison of techniques and implementation. *The Leading Edge*, 22(10), 942–953.
- Fazao, K.F., Djieto-Lordon, A.E., Ali, E.A.A., Agying, C.M., Ndeh, D.M. & Djuka, M.K., 2019. Analysis of shaly sand reservoir rocks in the eastern Niger Delta Basin using geophysical well logs. *Journal of Petroleum and Gas Engineering*, 10(1), 1–13. <https://doi.org/10.5897/JPGE2018.0300>.
- Ghosh, D., Sajid, M., Ibrahim, N.A. & Viratno, B., 2014. Seismic attributes add a new dimension to prospect evaluation and geomorphology offshore Malaysia. *The Leading Edge*, 33(5), 536–538.
- Hermana, M., Lubis, L.A., Ghosh, D.P. & Sum, C.W., 2016. New Rock Physics Template for Better Hydrocarbon Prediction. In *Offshore Technology Conference Asia* (pp. 22–25).
- Hermana, M., Ngui, J.Q., Sum, C.W. & Ghosh, D.P., 2018. Feasibility Study of SQp and SQs Attributes Application for Facies Classification. *Geoscience*, 8(10), 1–8. <https://doi.org/10.3390/geosciences8010010>.
- Joseph, E., Che, A., Ali, A., Adli, A., Mohd, Z. & Sali, S., 2019. An overview of 20 years' hydrocarbon exploration studies and findings in the Late Cretaceous-to-Tertiary onshore Central Sarawak, NW Borneo : 1997 – 2017 in retrospect. *Journal of Petroleum Exploration and Production Technology*, 9(3), 1593–1614. <https://doi.org/10.1007/s13202-018-0591-8>.
- Leveaux, J. & Poupon, A., 1971. Evaluation of Water Saturation in Shaly Formations. *The Log Analyst*, 12(4), 3–8.
- Shahud, N., Yeshpal & Singh, 2011. AVO Application for carbonates reservoir characterization in Sarawak Basin. *Petroleum Geology Conference and Exhibition*, (7-8<sup>th</sup> March 2011), Kuala Lumpur Convention Center.
- Vahrenkamp, V.C., 1998. Miocene carbonates of the Luconia province, offshore Sarawak: implications for regional geology and reservoir properties from Strontium-isotope stratigraphy. *Bulletin of the Geological Society of Malaysia*, 42, 1–13.
- Werthmüller, D., Ziolkowski, A. & Wright, D., 2013. Background resistivity model from seismic velocities. *Geophysics*, 78(4), E213 -E223.
- Zahra, A., Zailani, A. & Ghosh, D.P., 2017. Characterizing Geological Facies using Seismic Waveform Classification in Sarawak Basin. *Characterizing Geological Facies using Seismic Waveform Classification in Sarawak Basin*. *Earth and Environmental Science*, 88(012001).

*Manuscript received 16 December 2019*  
*Revised manuscript received 10 August 2020*  
*Manuscript accepted 1 September 2020*